Electrochemical etching process for Mg-Ca-Zn alloy

XIAOGANG JIA, YUAN HUANG, FANG HE*, LIFEN ZHANG, ZHAOHUI LU[a]
Tianjin University, Tianjin City, People's Republic of China, 300072
[a]Shanghai Children's Medical Center, shanghai, People's Republic of China, 200217

A new electrochemical etching method for the Mg-Ca-Zn alloy, including a new electrolyte solution and technological parameters, was developed in this paper. The EDTA in the electrolyte solution can chelate with Mg^{2+} and form the Mg-EDTA complex, which can play a crucial role in the selective etch. The lateral etching in the Mg-Ca-Zn alloy could be restrained while the vertical etching was enhanced through adjusting the stirring speed to obtain the reasonable electrolyte fluid field. In addition, surface fluorination treatment for the etched Mg-Ca-Zn alloy was also developed in this paper, which showed the corrosion behavior was improved.

(Received August 25, 2014; accepted November 13, 2014)

Keywords: Smelting, Electrochemical etching, Mg-Ca-Zn alloy, Surface fluorination treatment

1. Introduction

Magnesium alloys, as the lightest structure alloys, have received increasing research interests due to their high specific strength, excellent damping property, good electromagnetic shielding, and environmental friendly, etc.[1-7] Correspondingly, many processing methods used for magnesium alloys, including laser etching and die-casting, etc. have been reported in many literatures. For instance, laser etching was utilized to machining two types of magnesium alloy vascular stents by Biotronik Company [8]. Die-casting was used by White Metal Castin to produce several kinds of magnesium alloy computer casings [9]. However, these methods required a sophisticated computer - controlled equipment and computer programs, which are very complicated, high cost, and may damage original microstructures and properties of magnesium alloys [10].

Compared with the above methods, electrochemical etching was relatively simple, which do not need computer programs and expensive equipment. Electrochemical etching was usually used to create porous structure for some materials or machine alloy workpieces with special geometric patterns such as vascular stents, tourist souvenirs, medals, fine parts and so on. Tjerkstra et al [11] obtained porous GaP by anodic etching in H_2SO4 electrolyte. Mineta investigated the electrochemical etching characteristics of NiTi shape memory alloy using new electrolytes [12], this etching technique has been used for the fabrications of micro-actuators. The requirements of electrochemical etching processes for the processing materials were standard low potential, active chemical properties, bad corrosion resistance and the mild etching process. Magnesium alloys, including Mg-Ca-Zn alloy, were chemically active and easily corroded because of their low standard electrode potentials [13-15], which can fully meet the requirements.

Mg-Ca-Zn alloy was a new type of magnesium alloy developed in recent years, of which Ca can effectively refined grains, improve creep resistance, enhance the oxidation resistance of magnesium alloys at high temperatures and improve biocompatibility. When the dosage of Ca is 1%, the tensile strength and elongation rate of magnesium alloy reached the highest. Zn can improve the fluidity of alloy liquid, mechanical properties of magnesium alloys and the quality of casting. Due to the above characteristics, the alloy has potential applied value in biological materials field such as tracheal stent. Tracheal stent has very complex hollowed-out pattern and laser cut processing requires complex programming. According to the above, the electrochemical etching processing methods for the Mg-Ca-Zn alloy were set as the research target in this paper.

The difficulty of electrochemical etching processing method of Mg-Ca-Zn alloy mainly has two aspects: One is that, Mg-Ca-Zn alloy was chemically active and easily corroded simultaneously in all directions mainly lateral and vertical directions of the material, for which the specific geometric pattern etched was not easy to be obtained in the workpieces. Fig. 1 showed how the isotropic and anisotropic etching occurred respectively. Etch rates of isotropic etching on the etch profile in all directions (lateral and vertical) are same, which may produce side corrosion. To solve this problem, a reasonable formulation of electrolyte should be obtained first，then the etching in the lateral direction in the magnesium alloy could be restrained while the etching in the vertical direction be enhanced through adjusting the

etching process parameters. Another one is that, etched surface of Mg-Ca-Zn alloy will be eroded under long-term storage, the surface modification to improve the corrosion resistance was necessary. Traditional methods of surface modification to enhance the corrosion resistance of magnesium alloy includes anodic oxidation, ion implantation and coating technology etc. [16, 17], among which, fluoride treatments have been extensively reported [18]. The mechanism was that a thin protective magnesium fluoride layer can be rapidly formed on the etched surface as a result of the reaction between F^- and the α phase appearing during etching process [19, 20]. Hence, the surface fluorination treatment in NH_4F solution was choosed to modify the etched surface in this paper.

It turned out that Mg-Ca-Zn alloy specimens with designed patterns could be obtained.

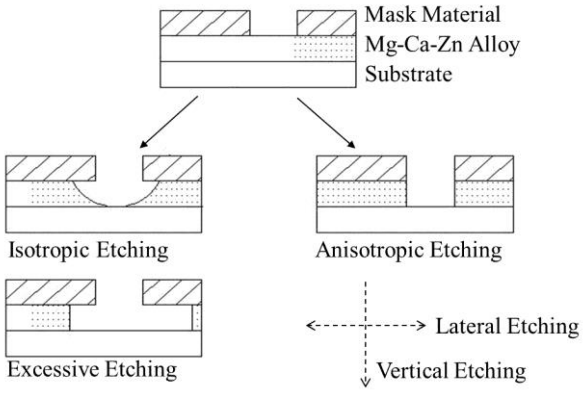

Fig. 1. The isotropic and anisotropic etching.

2. Experimental

The Mg-Ca-Zn alloy samples were first prepared through smelting, solution treatment and hot extrusion. The electrochemical etching was carried out in the new-designed electrolytic solution. Finally the surface fluorination treatment was implemented for the Mg-Ca-Zn alloy after electrochemical etching.

2.1. Preparation of Mg-Ca-Zn alloy

Mg-Ca-Zn alloy was fabricated by melting pure magnesium (99.98wt-%), calcium (99.98wt-%) and zinc (99.99wt-%) with weight ratio of 97.0: 1.0: 2.0 in the smelting furnace at 720°C for 30 minutes and subsequently casting at 680°C in a crucible-type of resistance furnace under a protective atmosphere of SF_6 and CO_2 (0.5: 99.5). After solution treatment at 330 °C for 6 h, the Mg-Ca-Zn alloy ingot was hot extruded in order to improve the plasticity and mechanical properties, during which the hot extrusion temperature was 300~320°C, hot extrusion speed was 10mm/s and hot extrusion ratio (Δ) was 16. The as-extruded Mg-Ca-Zn alloy was cut into sheets with different sizes. Then the sheets were abraded on SiC papers (grit 400 and 2000 sequentially) and polished with the Al_2O_3 (50 nm) slurry. Then the Mg-Ca-Zn alloy sheets were ultrasonically cleaned in a 1:1 mixture of ethanol and acetone for 10 min.

The optical microstructures of Mg-Ca-Zn alloy were observed under a metallurgical microscope (OLYMPUS BX41M). EDS (Genesis XM2) analysis was used to determine the actual composition of the Mg-Ca-Zn alloy. X-ray diffraction (XRD, RIGAKU/DMAX) analysis was used to characterize the phase constituents of the alloys. The tension test for the Mg-Ca-Zn alloys, including the samples with hot extrusion and the samples without hot extrusion, were conducted using electronic universal testing machine. The characterization of the microstructure of the Mg-Ca-Zn alloys' tensile fracture was carried out using scanning electron miscopy (SEM, Hitachi FE-SEM S4800 manufactured by Hitachi Company).

2.2 Preparation of electrolytic solution

Electrolytic solution was designed and prepared by dissolving solutes in the deionized water with magnetic stirring at 30°C, and the composition of electrolytic solution was given in Table 1. Since magnesium and magnesium alloys were very active metals, which could be corroded in alkaline conditions, so the suitable dosage of NaOH was necessary. Na_2SiO_3 acted as a corrosion inhibitor, which alleviated the Mg-Ca-Zn alloy's natural corrosion. Ethylene Diamine Tetraacetic Acid (EDTA) can chelate with $Mg^{2+}$and form a stable complex compound (Mg-EDTA complex), which can make the corrosion rate decreased. This complex was the key material to make the etching in lateral direction in the Mg-Ca-Zn alloy could be restrained while the etching in the vertical direction was enhanced. The complex reaction was shown in equation (1). $NaNO_2$ acted as a precursor in the solution，and the effect was shown in equation (2). NH_4F can slow down the oxidation reaction speed and prevent the formation of pitting.

$$Mg^{2+} + EDTA \rightarrow Mg\text{-}EDTA \quad (1)$$

$$NO_2^- + H_2O \rightarrow HNO_3 + H^+ + 2e \quad (2)$$

Table 1. Nominal composition of electrolytic solution/mol/L.

Electrolytes composition	$NaNO_2$	NaOH	Na_2SiO_3	NH_4F	EDTA
Concentration	0.50	0.10	0.01	0.01	0.01

2.3 Pre-preparation of samples before etching

Double-sided scotch tape was used as the mask material, which was comprised of three layers: basematerial, adhesive, and release paper. The adhesive

consists of various polymers, such as epoxy, polypropylene, etc. which could form firm bonding with the Mg-Ca-Zn alloy and protect the covering parts from being etched in the electrolytic solution. The mask processing was carried out as follows: one side of the specimen was entirely protected with the tape, and the other side covered by the tape with specified patterns as shown in Fig. 2*b* faced the cathode. Fig. 2*a* showed the side view of Mg-Ca-Zn sheet. This mask process could realize the only etching of unprotected part of the sample.

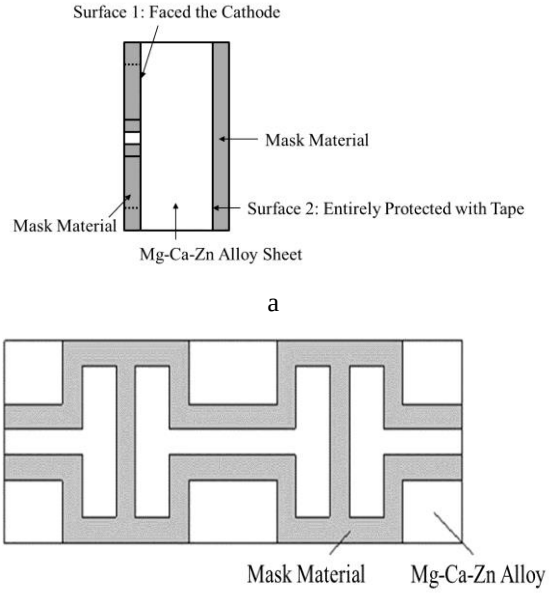

Fig. 2. a) side-view of mask process, b) top view of mask process.

2.4 Electrochemical etching setup and conditions

Electrochemical etching was carried out using the setup as shown in Fig. 3. A two-electrode configuration voltage was applied between the Mg-Ca-Zn sheet anode and the counter cathode of an Ag plate. Both electrodes were facing each other with a gap of 40 mm in the electrolyte solution (200 ml). The applied voltage was 8 V and the temperature was maintained at 30°C under magnetic stirring during electrochemical etching process. After the electrochemical etching, the mask material was removed.

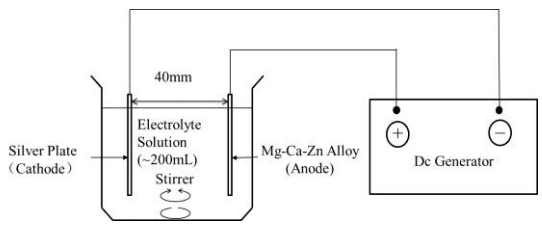

Fig. 3. Setup for electrochemical etching of the Mg-Ca-Zn alloy.

2.5 Surface fluorination treatment of etched samples

Due to the lively chemical properties and bad carrion resistance of Mg-Ca-Zn alloy, the surface treatment of as-etched Mg-Ca-Zn alloy was necessary. In this study, surface fluorination treatment was used to generate the corrosion resistant layer on the etched surface of the Mg-Ca-Zn alloy. Once the etch of the samples finished, they were chemically treated by completely steeping in 2.5 mol L^{-1} NH_4F solution of pH 6.0 ± 0.5 at 75 ± 5°C for 20 minutes. Then the samples were rinsed with deionization water and stored in high purity ethyl alcohol (99.9wt-%) at room temperature.

The SEM equipped with EDS and XRD were used to investigate the surface morphologies and the phase of the etched specimens. Electrochemical measurements were carried out using a potentiostat PARSTAT 2273 from Princeton Applied Research with the help of the POWERSUIT software, where the potential range of polarization curves was ± 1 V with a scan rate of 1 mV s^{-1}. A standard three-electrode cell was set up to conduct the potentiodynamic polarization test. Saturated calomel and platinum electrodes were used as the reference and counter electrodes.

3. Results and discussion

3.1 Properties of as-prepared Mg-Ca-Zn alloys

The actual compositions of the Mg-Ca-Zn alloy obtained from the EDS analysis were shown in Table 2.

Table 2. Nominal chemical compositions of Mg-Ca-Zn alloy/wt-%.

Mg	Ca	Zn	O	C
94.75	1.12	2.06	1.02	1.05

The XRD analysis of Mg-Ca-Zn alloy (including the un-extruded and extruded samples) was shown in Fig. 4. From Fig. 4, in addition to Mg peaks, the diffraction peaks associated with Mg_2Ca and $Mg_6Ca_2Zn_3$ phases were also observed in the diffraction spectrums, which was in good agreement with the Mg-Ca-Zn three binary alloy phase diagram at 300°C [21]. The optical microstructures of Mg-Ca-Zn alloy (including the un-extruded and extruded samples) were shown in Fig. 5. Fig. 5*a* showed the optical microstructures of Mg-Ca-Zn alloy samples after solution treatment with un-extrusion, and the optical microstructures of Mg-Ca-Zn alloy after solution treatment and hot extrusion were showed in Fig. 5*b*. In Fig. 5*a*, Mg constituted the entire matrix organization, the fine

particulate phase was Mg_2Ca, and the discontinuous reticular distribution phase was $Mg_6Ca_2Zn_3$. Fig. 5*b* shows the same distribution of various phases. Obviously, the hot extrusion process applied in this paper didn't change the phase in the Mg-Ca-Zn alloy.

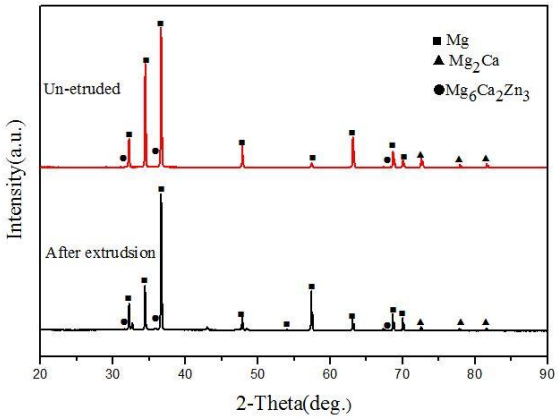

Fig.4. X-ray diffraction patterns of Mg-Ca-Zn alloy samples.

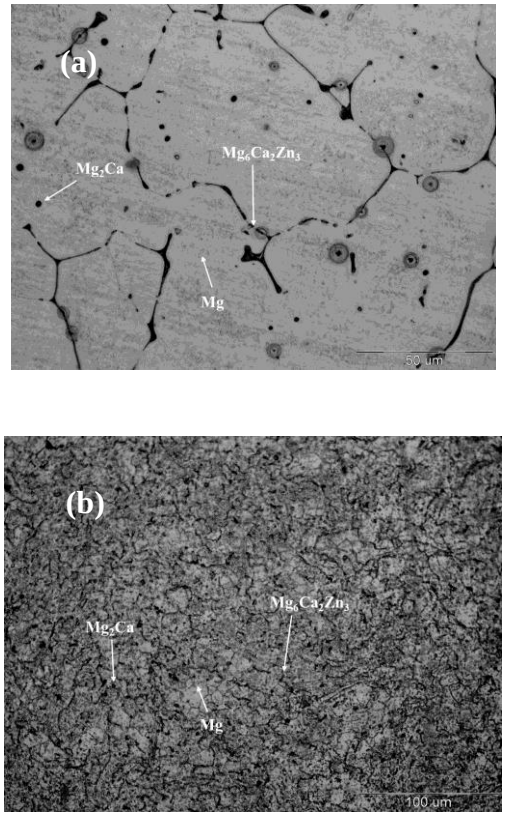

Fig. 5 a the optical microstructures of Mg-Ca-Zn alloy samples after solution treatment with un-extrusion, b Mg-Ca-Zn alloy after solution treatment and extrusion; samples were etched with 4% nital.

Fig. 6 showed the tensile curves of the Mg-Ca-Zn alloy samples before and after hot extrusion and the SEM photos of tensile fracture after hot extrusion. The mechanical properties of alloy obtained from the tensile curves were shown in Table 3, from which it could be seen that the tensile mechanical properties of Mg-Ca-Zn alloy have been improved through the hot extrusion. It could be also seen that the yield platform appeared on the tensile curve that represented the hot-extruded sample. Fig. 6*b* was the SEM photos of the tensile fracture of the hot-extruded sample, where it could be seen that there were a lot of dimples in the tensile fracture. All those showed that the Mg-Ca-Zn alloy has good plasticity and strength after hot extrusion. So, the Mg-Ca-Zn alloy obtained in this study will be used to conduct the electrochemical etching.

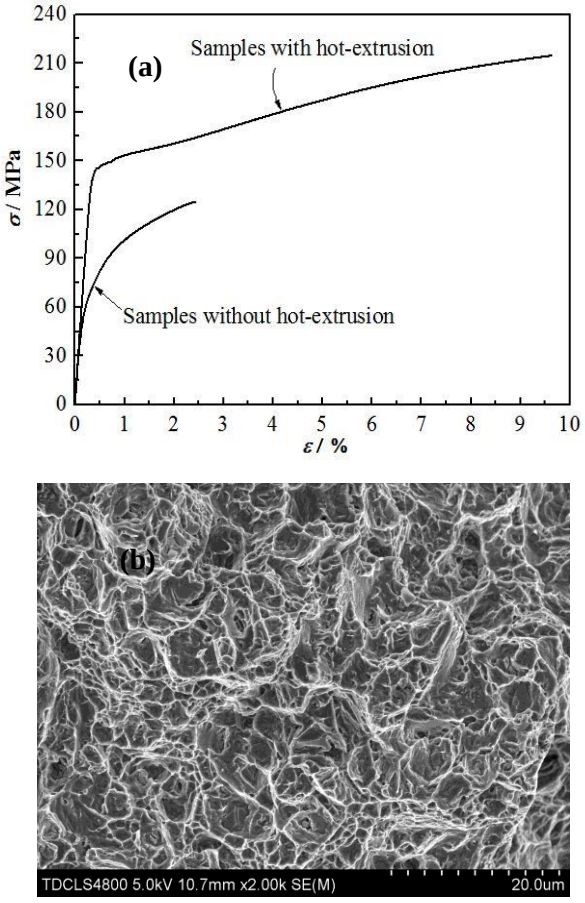

Fig. 6. a tensile stress-strain curves of Mg-Ca-Zn alloys, b image (SEM) of the tensile fracture of the sample with the extrusion.

Table 3. The tensile properties of extruded Mg-Ca-Zn alloy.

Properties	**E/GPa**	**Rm/MPa**	**F_b/N**
Sample without hot extrusion	42.55	124.5	1689.4
Sample with hot extrusion	45.12	229.0	3156.8

3.2 Mechanism of etching for Mg-Ca-Zn alloy

Fig. 7*a* was the photograph of etched Mg-Ca-Zn metal sheets with different patterns obtained in this paper; obviously, the method was a quite practical way. It could also be noticed that the samples etched have smooth surface and straight edge (Fig. 7*b*). All these implied that the etching is anisotropy：etching in the lateral direction in the Mg-Ca-Zn alloy can be restrained while the etching in the vertical direction can be enhanced.

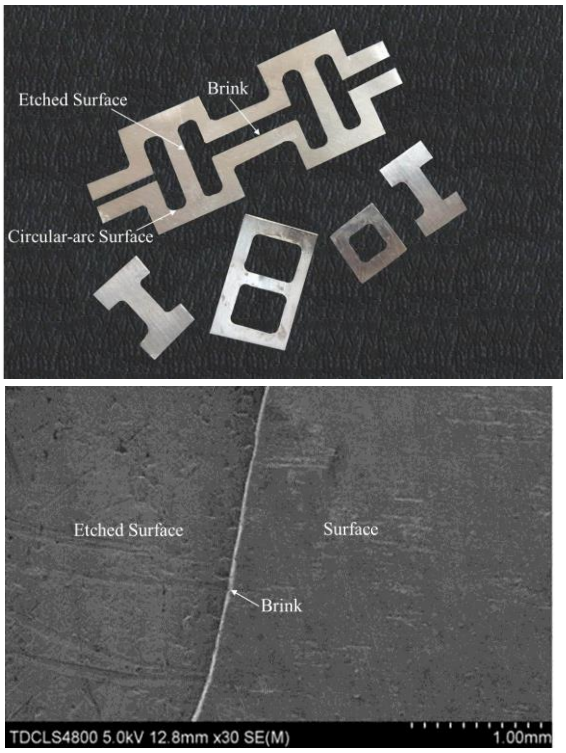

Fig. 7. a photographs of etched patterns, b image (SEM) of the etched surface.

In order to investigate the etching mechanism, the pH curve of the electrolytic solutions changing with the etching time was measured and the result was shown in Fig. 8, from which it can be noticed that the pH value rise and is higher than 10 after 600 seconds. Meanwhile, there was a kind of white precipitates appearing in the solution after a few minutes of etching of the Mg-Ca-Zn alloy. Combined with the literature [22], the precipitates should be mainly $Mg(OH)_2$. The overall reaction of the etching process was concluded as shown in equation (3):

$$Mg^{2+} + 2H_2O \rightarrow Mg(OH)_2 \downarrow + H_2 \uparrow \quad (3)$$

The step chemical reaction process was as follows:

$$Mg \rightarrow Mg^{2+} + 2e \quad (4)$$

$$2H_2O + 2e \rightarrow H_2 \uparrow + 2(OH)^- \quad (5)$$

$$NaOH \rightarrow Na^+ + (OH)^- \quad (6)$$

$$Mg^{2+} + 2(OH)^- \rightarrow Mg(OH)_2 \downarrow \quad (7)$$

It was because the OH^- produced in the reaction shown in the equation (5, 6) that the pH value rose. At higher pH value, Mg^{2+} could chelate with EDTA and form one kind of stable complexes (Mg-EDTA Complex) according to the literature (equation (2)) [23].

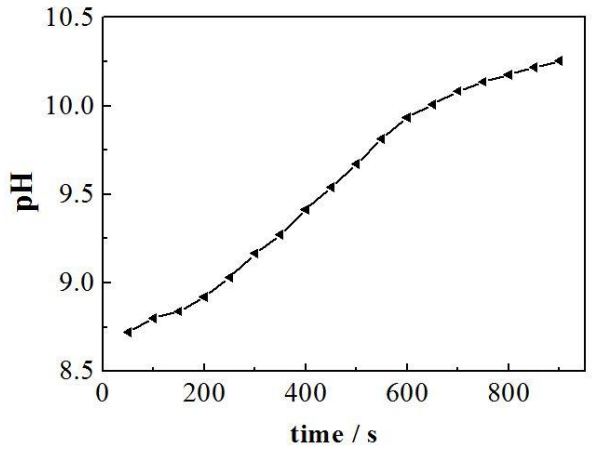

Fig. 8. The pH change of the electrolyte solution along with electrochemical duration.

The Mg-EDTA complex could restrain the etching. The viscosity of the electrolyte was small and the etched-groove formed on the sample surface in the first few minutes of etching process. Fig. 9a showed the perspective view of the mechanism diagram of electrochemical etching. After the etched-groove formed, the electrolyte should flow in the etched-groove as shown in Fig. 9b according to the arrangement of the stirrer (see Fig. 3). According to fluid mechanics [24], the electrolyte fluid field in the etched-groove can be divided into three areas. Area I (The main stream area of the fluid): The electrolyte flowed into the etched-groove along the tangential direction with fast flow velocity under stirring. And the flow velocities of the electrolyte solution were distributed in descending order from top to bottom of the etched-groove. Because the etched-groove was shallow, the electrolyte near the bottom of the etched-groove still had a large velocity when the stirring speed was appropriate, from which the Mg-EDTA complex cannot gather at the bottom side of the etched-groove, which can ensure that the etching in vertical direction occur. If the flow velocity of the electrolyte was faster, the etching in vertical direction should be enhanced. Area II (Stagnation area): The flow velocity of the electrolyte in this area was small. The flow velocity of the electrolyte closed to the lateral sides of the etched-groove was almost 0 when the stirring speed was appropriate. The Mg-EDTA complex could gather near the side wall, which could effectively restrain the etching in the lateral direction. Area III (Induced eddy area): Induced eddy would form in the bottom corner of the etched-groove and the flow velocity of the electrolyte in this area was small. Although the Mg-EDTA complex

could also gather here, the electrolyte could cause slight etching which caused a circular-arc surface, proven by the masked area in Fig. 7a.

The following conclusions were drawn from the experimental results and discussion above. To restrained completely lateral etching, enhance the vertical etching and eliminate the circular-arc surface, subsequent research should be carried out as following two aspects: (1) Design electrolyte to produce a more effective complex during the etch process; (2) Design a more reasonable arrangement of the stirrer to make the flow velocity of the electrolyte at the bottom of the etched-groove be more faster and the flow velocity along the lateral sides of the etched-groove be more slower and the induced eddy be eliminated.

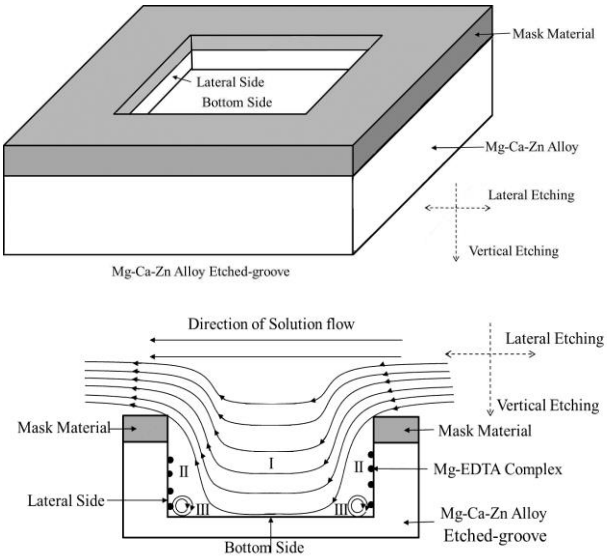

Fig. 9. a perspective view and b cross-sectional view of the mechanism diagram of electrochemical etching.

3.3 Affecting factors for etching process

During the etching process, the etching rate of the samples in electrolytic solutions was influenced mainly by two principal factors: the etching temperature and the stirring speed. The research results of the effects of the two factors on the etching rate (weight loss) were shown in Fig. 10. From Fig. 10*a*, the etch rate rises slightly with the increasing temperature. When the temperature went up to 30^{o}C (curve *c* in Fig. 10*a*), the weight loss rises almost linearly with time, which meant that the etching rate is uniform. The etching temperature was too low or too high would all lead to obtain obscure patterns in the experiments. The reason was that high temperature will decrease the adhesion strength between the mask material and the surface of the Mg-Ca-Zn alloy, and low temperature will slow down the formation reaction of Mg-EDTA complex, which lead the lateral etching can't be restrained.

Meanwhile, the stirring speed was also a very important factor during the etching process, which made the surface not be oxidized and the etching rate not disturbed by the generated material [25]. Fig. 10*b* shows that the etch rate also rose with the increasing stirring speed, where it could be noted that the etching rate was the most stable at the stirring speed of 50r/s (curve *b* in Fig. 10*b*). The stirring speed was too low would lead the etching efficiency to be too slow, conversely, too fast would lead to obtain obscure edge in the patterns in the experiments. The reason was that fast stirring speed will cause the Mg-EDTA complex to be unable to deposit or gather on the lateral sides, thus, the lateral etching can't be restrained.

From the analysis above, the most suitable etching temperature was 30°C, and the most suitable stirring speed was 50r/s in this study.

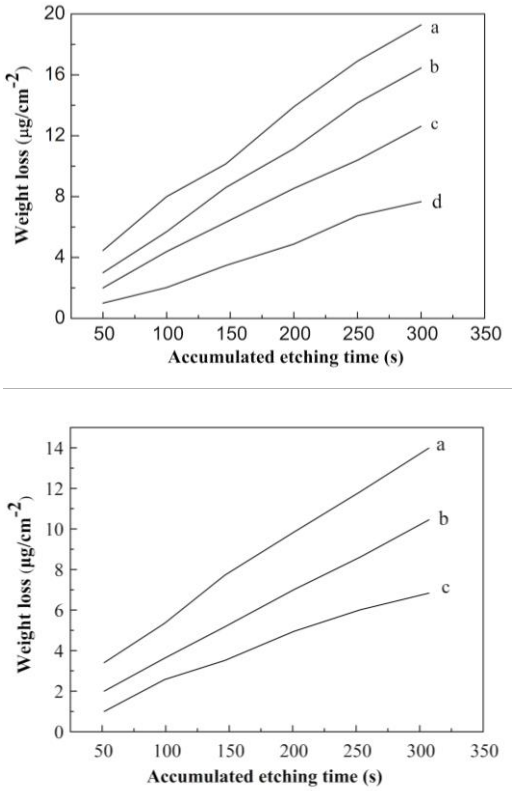

Fig. 10. a weight losses for Mg-Ca-Zn alloy in different temperatures: a 50 ℃, b 40 ℃, c 30 ℃, and d 20 ℃, and b at different stirring speeds: a 100 r/s, b 50r/s, and c 0 r/s.

3.4 Surface fluorination treatment of etched samples

The etched surface of non-treated sample has been shown in Fig. 7*b*. Fig. 11 showed the surface morphology of the etched Mg-Ca-Zn alloy samples after the surface fluorination treatment. After being treated, a net structured layer formed and evenly covered on the etched surface

(Fig. 11). By comparison Fig. 7*b* with Fig. 11, it is clearly seen that the net structured layer is more compact. Superimposed on the image (Fig. 11) are EDX spectrum of the local region of the net structure, which shown two characteristic peaks, respectively, on behalf of the Mg and F elements, proving the formation of magnesium fluoride network layer [26].

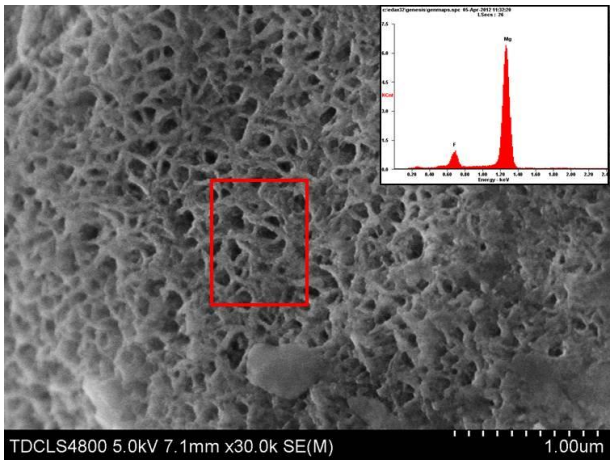

Fig. 11. Images (SEM) of etched surface after the fluorination treatment, the insert was the corresponding EDAX analysis.

To confirm the increase of the corrosion resistance of the etched samples after surface fluorination treatment, the electrochemical measurements were carried out in a 3.5% NaCl solutions at room temperature. The potentiodynamic polarization curves of etched surface obtained were shown in Fig. 12, where curve *a* represented the samples without the surface fluorination treatments and curve *b* represented the samples with the treatments. As can be seen from Fig. 12, the electrochemical corrosion potential after surface fluorination treatment increased obviously, the corrosion potential of the curve *a* was about 80mv which is lower than that of the curve *b*. In addition, the corrosion current density of the curve *a* was about 1A higher than that of the curve *b*. Generally speaking, it is beneficial in the polarization test that the corrosion potential is much higher and the corrosion current density is much lower. Therefore a conclusion could be made that the dense reticular layer which formed on the surface of the etched Mg-Ca-Zn alloy after the surface fluorination treatment can effectively prevent the formation of free Mg^{2+} from the Mg-Ca-Zn alloy, make corrosion potential of the Mg-Ca-Zn alloy rise and cause the corrosion depth and rate decrease, which greatly improved the corrosion resistance of the surface of the etched Mg-Ca-Zn alloy.

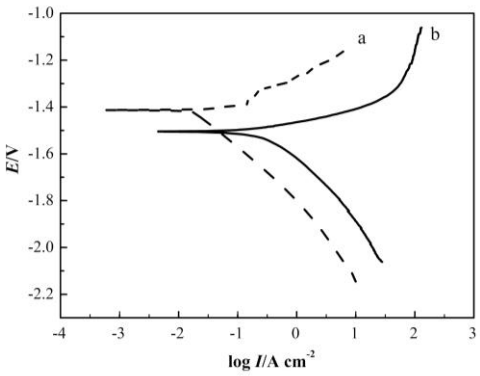

Fig. 12. Potentiodynamic polarization curves of etched surface a before and b after the surface fluorination treatments in 3.5% NaC1 solution at 25 ℃.

4. Conclusions

In the present work, the electrochemical etching method for the Mg-Ca-Zn alloy was analysed. The following conclusions were drawn from the experimental results and discussion.

1. The electrochemical etching processing method used to obtain the Mg-Ca-Zn alloy samples with complex hollow-out patterns was feasible. Compared with the laser etching, die-casting, etc. the electrochemical etching was relatively simple and inexpensive.

2. A new electrolyte solution was designed to produce the Mg-EDTA complex for etching Mg-Ca-Zn alloy. The Mg-EDTA complex can played a crucial role in the selective etch of the Mg-Ca-Zn alloy samples.

3. Lateral etching could be restrained and vertical etching be enhanced through adjusting the arrangement of the stirrer and stirring speed to form the reasonable electrolyte fluid field in the etched-groove, during which electrolyte could form the main stream area with large flow velocity in the vertical etching region and form the stagnation area in the lateral etching region, while eliminating the induced eddy in the bottom corner of the etched-groove.

4. The net structured magnesium fluoride layer evenly formed on the etched surface by the surface fluorination treatment, which was confirmed to improve the corrosion resistance of Mg-Ca-Zn alloy significantly by electrochemical tests.

Acknowledgments

This study was supported by the National Natural Science Foundation of China (NFSC) (project no. 30972960/H0106).

References

[1] X. Chen, J. Liu, Z. Zhang, F. Pan, Mater. Des., **42**, 327 (2012).
[2] T. Liu, F. Pan, X. Zhang, Mater. Des., **43**, 572 (2012)
[3] S. W. Xu, K. Oh-ishi, S. Kamado, F. Uchida, T. Homma, K. Hono, Scr. Mater., **65**(3), 269 (2011).
[4] M. B. Yang, F. Pan, L. Cheng, J. Shen, Mater. Sci. Eng. A., **A512**(1), 132 (2009).
[5] A. A. Luo, J. Magnesium Alloys, **1**, 2 (2013).
[6] P.-L. Mao, J.-C. Yi, Z. Liu, Y. Dong, J. Magnesium Alloys, **1**, 64 (2013).
[7] J. Zhang, W. Li, Z. Guo, J. Magnesium Alloys, **1**, 31 (2013).
[8] X. P. Wang, F. Z. Cui, J. G. Li, X. S. Zhao, Biomed. Eng., **26**(2), 338 (2009).
[9] J. A. Liu, Light Alloy Fabrication Technol., **29**, 1 (2001).
[10] L. M. Jiang, Z. Q. Tian, Z. F. Liu, B. W. Mao, H. G. Huang, J. J. Sun, Electrochem., **8**, 139 (2002).
[11] R. W. Tjerkstra, J. G. Rivas, D. Vanmaekelbergh, J. J. Kelly, Electrochem. Solid. State. Lett., **5**(5), G32 (2002).
[12] T. Mineta, J. Micromech. Microeng., **14**(1), 76 (2004).
[13] J. Martin, P. Dan, L. Christofer, Corros. Sci., **50**(5), 1406 (2008).
[14] S. Mathieu, C. Rapin, J. Steinmetz, P. Steinmetz, Corros. Sci., **45**(12), 2741 (2003).
[15] N. Pebere, C. Riera, F. Dabosi, Electrochim. Acta., **35**(2), 555 (1990).
[16] X. M. Wang, X. Q. Zeng, G. S. Wu, S. S. Yao, Y. J. Lai, J. Alloys. Compd., **437**(1), 87 (2007).
[17] M. Abulsaina, A. Berkania, F. A. Bonillaa, Y. Liua, M. A. Arenasa, P. Skeldon, G. E. Thompsona, T. C. Q. Noakesb, K. Shimizuc, H. Habazakid, Electrochim. Acta., **49**(6), 899 (2004).
[18] S. Verdier, N. V. Laak, S. Delalande, J. Metson, F. Dalard, Appl. Surf. Sci., **235**(4), 513 (2004).
[19] J. E. Gray-Munro, B. Luan, L. Huntington, Appl. Surf. Sci., **254**(9), 2871 (2008).
[20] J. Z. Li, J. G. Huang, Y. W. Tian, C. S. Liu, T. Nonferr. Met. Soc., **19**(1), 50 (2009).
[21] C. M. Liu, X. R. Zhu, H. T. Zhou, 186-187; 2006, Changsha, Central South University Press.
[22] J. C. Gao, S. Wu, L. Y. Qiao, Y. Wang, Trans. Nonferr. Met. Soc., **18**(3), 588 (2008).
[23] Z. P. Feng, J. Sou. Agr. Coll., **2**, 75 (1985).
[24] O. Herbert, 2010, New York, Springer-Verlag New York Inc.
[25] Y. Seikoh, Cryst. Growth., **181**(3), 293 (1997).
[26] M. C. Turhan, R. Lynch, M. S. Killian, S. Virtanen, Electrochim. Acta., **55**(1), 250 (2009).

*Corresponding author: hefang111222@163.com